Supporting Information

A Quantitative Mechanistic PK/PD Model Directly Connects Btk Target Engagement and *In Vivo* Efficacy

Fereidoon Daryaee[a,1], Zhuo Zhang[a,1], Kayla R. Gogarty[a], Yong Li [a], Jonathan Merino[a], Stewart L. Fisher[b,2] and Peter J Tonge[a,2]

[a]Institute for Chemical Biology & Drug Discovery, Department of Chemistry, Stony Brook University, Stony Brook NY 11794-3400

[b]C4 Therapeutics, Cambridge, MA 02142

[1]These authors contributed equally to this work.

[2]Authors to whom correspondence should be addressed:
SLF: stewfisher@slfisherconsulting.com; PJT: peter.tonge@stonybrook.edu

SI Materials and Methods

Synthesis of BDP-CC-292 (5), a fluorescent analog of CC-292

A covalent fluorescent Btk probe, BDP-CC-292, was synthesized from CC-292 as shown in **Scheme S1**. This method involved the synthesis of an azide derivative of CC-292 that was subsequently coupled to an alkyne analog of the fluorescent dye BODIPY using click chemistry. Each intermediate was purified by flash column chromatography and characterized by ESI-MS, ^{1}H and ^{13}C NMR. The final probe was purified by HPLC and characterized by ESI-MS.
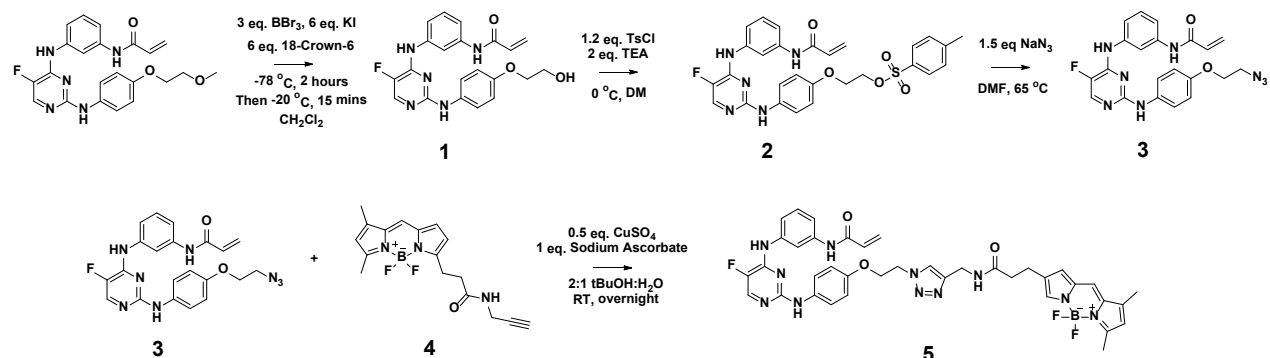
Scheme S1. Synthesis of BDP-CC-292 (**5**)

Demethylated CC-292 (1)

A solution of CC-292 (AVL-292, Ontario Chemicals Incorporated, 98% purity, CAS # 1202757-89-8) in 1 mL DCM was stirred at -80 ℃ for 5 min after which 120 mg of potassium iodide (KI) and 190 mg 18-Crown-6 were added. BBr$_3$ was dissolved in 1 mL of DCM and cooled to -80 ℃. The solution of BBr$_3$ in DCM was then added dropwise to the solution of CC-292 which was stirred continuously. After stirring for 1 h at -80 ℃, the mixture was warmed to -20 °C and stirred for another 15 min. Upon completion of the reaction, which was confirmed by TLC, the reaction was quenched by the addition of 2 mL saturated NaHCO$_3$ solution. The quenched reaction was stirred at RT for 10 min before the mixture was concentrated by rotary evaporation. The residual solution was extracted with 50 mL EtOAc for 3 times, and the organic layers were combined and then dried with MgSO$_4$. Evaporation under vacuum yielded crude product (**1**) which was purified by CombiFlash chromatography using a silica column.

ESI MS Calculated for C$_{21}$H$_{20}$FN$_5$O$_3$ *m/z* [M+H]$^+$ 410.16, found 410.1, ^{1}H NMR (400 MHz, Methanol-*d$_4$*) δ ppm 3.85 (t, *J*=4.80 Hz, 2 H), 4.00 (t, *J*=4.80 Hz, 2 H), 5.78 (dd, *J*=9.41, 2.13 Hz, 1 H), 6.33 - 6.40 (m, 1 H), 6.40 - 6.48 (m, 1 H), 6.80 - 6.86 (m, 2 H), 7.25 - 7.30 (m, 1 H), 7.38 - 7.45 (m, 4 H), 7.87 (d, *J*=4.02 Hz, 1 H), 8.05 (t, *J*=2.00 Hz, 1 H). ^{19}F NMR (376 MHz, Methanol-*d$_4$*) δ ppm -168.86 (s., 1F).

CC-292-Tosylate (2)

Demethylated CC-292 (**1**) (10 mg), 0.01 mL triethylamine (TEA) and 1 mg DMAP were added to a 10 mL RBF containing 0.5 mL DCM. The mixture was cooled to 0 ℃ and then stirred for 5 min. 4-Toluenesulfonyl chloride (TsCl) was dissolved in 0.5 mL DCM in a glass vial and cooled to 0 ℃. The TsCl solution was then added to the solution of **1** dropwise at 0 ℃, which was then stirred at 0 ℃ for 10 min and then warmed to RT. The reaction mixture was stirred for another 12 h and when the reaction was shown to be complete by TLC the solution was evaporated under vacuum. Crude product (**2**) was obtained as a yellow residue and used in the next step without further purification.

Azido-CC-292 (3)

Crude CC-292-Tosylate (**2**) (13 mg) was added to a 10 mL RBF containing 0.5 mL DMF and 3 mg NaN_3. The mixture was stirred at 65℃ overnight and iced cold water was added after TLC demonstrated that the reaction was complete. The aqueous mixture was extracted with 10 mL EtOAc for 3 times and the organic layers were combined and dried with $MgSO_4$. After filtering, the solvent was evaporated under vacuum and the crude solid product was purified by CombiFlash chromatography using a silica column.

ESI MS Calculated for $C_{21}H_{19}FN_8O_2$ m/z [M+H]$^+$ 435.44, found 435.1, ^{1}H NMR (400 MHz, Methanol-d_4) δ ppm 3.85 (t, J=4.80 Hz, 2 H), 4.00 (t, J=4.80 Hz, 2 H), 5.78 (dd, J=9.41, 2.13 Hz, 1 H), 6.33 - 6.40 (m, 1 H), 6.40 - 6.48 (m, 1 H), 6.80 - 6.86 (m, 2 H), 7.25 - 7.30 (m, 1 H), 7.38 - 7.45 (m, 4 H), 7.87 (d, J=4.02 Hz, 1 H), 8.05 (t, J=2.00 Hz, 1 H). ^{19}F NMR (376 MHz, Methanol-d4) δ ppm -168.74 (d, J=4.09 Hz). ^{13}C NMR (126 MHz, Methanol-d_4) δ ppm 50.04, 67.27, 113.78, 114.30, 115.41, 117.62, 121.39, 126.58, 128.55, 131.13, 134.07, 138.49, 139.12, 139.47 (d, J=20.89 Hz, 1 C), 140.69 (d, J=246.14 Hz, 1 C), 150.55 (d, J=10.90 Hz, 1 C), 153.86, 156.17 (d, J=2.73 Hz, 1 C), 164.72.

BDP-CC-292 (5)

Azido-CC-292 (**3**) (0.5 mg) and 0.5 mg BDP FL alkyne (**4**, purchased from Lumiprobe) were added to a 1.5 mL glass reaction vial after which 0.2 mL tBuOH was added. Sodium ascorbate (2.3 mg) was dissolved in 0.5 mL H_2O and 1.4 mg $CuSO_4·5H_2O$ was dissolved in 0.1 mL H_2O. Subsequently, 0.05 mL of each solution was added by pipette to the glass vial containing 0.2 mL tBuOH, Azido-CC-292 (**3**) and BDP FL Alkyne (**4**). The reaction mixture was stirred at room temperature overnight, filtered and then purified by HPLC using an analytical PFP column (Phenomenex, PFP, 250 × 4.6, 5 μm). Chromatography was performed at a flow rate of 0.8 mL/min using a gradient of 0.020 M NH_4OAc in H_2O and MeCN. The mobile phase consisted of 0% MeCN (0 to 5 min), 0 to 50% MeCN (5 to 30 min), 50 to 100% MeCN (30 to 50 min), 100 to 0% MeCN (50 to 60 min). The pure product (**5**) eluted at 35.5 to 37.5 min and was characterized by ESI-MS and NMR spectroscopy.

ESI MS Calculated for $C_{38}H_{37}BF_3N_{11}O_3$ m/z [M+H]$^+$ 764.31, found 764.3, m/z [M+Na]$^+$ 786.31, found 786.3, HR MS Calculated for $C_{38}H_{37}BF_3N_{11}O_3$ m/z [M+H]$^+$ 764.31, found 764.3193.
^{1}H NMR (500 MHz, DMSO-d_6) δ ppm 1.24 (s., 3 H), 2.36 - 2.38 (m, 2 H), 2.41 (s, 3 H), 2.64 - 2.65 (m, 2 H), 4.29 - 4.35 (m, 4 H), 4.69 - 4.72 (m, 2 H), 5.76 (s., 1 H), 6.33 (d, J=3.81 Hz, 1 H), 6.36 (d, J=3.20 Hz, 1 H), 6.53 (s, 1 H), 6.75 (d, J=9.46 Hz, 2 H), 7.05 (d, J=4.27 Hz, 1 H), 7.10 (s, 1 H), 7.12 - 7.19 (m, 3 H), 7.38 - 7.44 (m, 2 H), 7.48 - 7.56 (m, 3 H), 7.88 (d, J=11.90 Hz, 1 H), 8.09 (s, 1 H)

Equilibrium target occupancy (MATLAB)

CC-292 is an irreversible inhibitor of Btk which binds to the ATP binding site (**Scheme S2**).
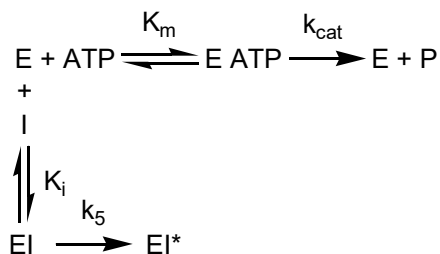
Scheme S2. Kinetic scheme for the reaction of Btk with an irreversible competitive inhibitor.

A model that correlates target occupancy with inhibitor concentration ([I]) at equilibrium was derived assuming the steady-state approximation for enzyme-substrate turnover, rapid equilibrium for initial

enzyme-inhibitor complex formation, and that negligible target degradation and re-synthesis occurred during the exposure of the cells to the inhibitor.

According to mass balance:

$$E_0 = E_t + ES + EI + EI^*$$

Therefore:

$$E_0 = E_t + E_t * \left(\frac{S}{K_m}\right) + E_t * \left(\frac{I}{K_i}\right) + EI^*$$

Rearrangement gives:

$$E_0 = E_t * \left(1 + \frac{S}{K_m} + \frac{I}{K_i}\right) + EI^*$$

If $\alpha = \left(1 + \frac{S}{K_m} + \frac{I}{K_i}\right)$

Then:

$$E_t = \frac{E_0 - EI^*}{\alpha}$$ **Eq. S1**

According to drug-target kinetics:

$$\frac{dEI^*}{dt} = k_5 * EI = k_5 * E_t * \left(\frac{I}{K_i}\right)$$

$$\frac{dEI^*}{dt} = \left(\frac{k_5 * I}{K_i}\right) * \left(\frac{E_0 - EI^*}{\alpha}\right)$$

and since $K_i * \alpha = K_i^{app} + I$
Therefore:

$$\frac{dEI^*}{dt} = \left(\frac{k_5 * I}{K_i^{app} + I}\right) * (E_0 - EI^*)$$

If $b = \left(\frac{k_5 * I}{K_i^{app} + I}\right)$

$$\frac{dEI^*}{dt} = -b * (-E_0 + EI^*)$$

Solution of the above differential equation yields:

$$EI^* = EI_0^* * e^{-b*t} + E_0 * \left(1 - e^{-b*t}\right)$$

Given that in the cellular target occupancy experiment, the initial concentration of irreversible enzyme-inhibitor complex is zero:

$$EI^* = E_0 * \left(1 - e^{-b*t}\right)$$

Therefore, target occupancy (TO) is defined as:

$$TO = \frac{EI^*}{E_0} = 1 - e^{-b*t}$$ **Eq. S2**

and so:

$$TO = 1 - e^{-\left(\frac{k_5*I}{K_i^{app}+I}\right)*t}$$ **Eq. S3**

Model for cellular and *in vivo* target occupancy (MATLAB)

The concentrations of E, ES, EI and EI* change over time as expressed by differential **Eq. S4 to S8**.

$$\frac{dE_t}{dt} = -k_3 * [I] * E_t + k_4 * EI - k_1 * [S] * E_t + k_2 * ES + k_{cat} * ES$$ **Eq. S4**

$$\frac{dE.S}{dt} = k_1 * [S] * E_t - k_2 * ES - k_{cat} * ES$$ **Eq. S5**

$$\frac{dP}{dt} = k_{cat} * ES$$ **Eq. S6**

$$\frac{dE.I}{dt} = k_3 * [I] * E_t - k_4 * EI - k_5 * EI$$ **Eq. S7**

$$\frac{dE.I^*}{dt} = k_5 * EI$$ **Eq. S8**

In which, $E_{t=0}$ = E_0; $ES_{t=0}$ = 0; $P_{t=0}$ = 0; $EI_{t=0}$ = 0 and EI*$_{t=0}$ = 0, and [S]=substrate concentration ([ATP]) which is assumed to be constant, and [I]= inhibitor concentration which is assumed to be constant in the cellular assays and to be the serum free fraction for the *in vivo* experiments.

Dividing both sides of **Eq. S4-S8** by [E_0] yields the relative fraction for each of the enzyme species.

From mass balance: $E_0 = E + ES + EI + EI^*$

so $E = E_0 - ES - EI - EI^*$

Converting the above mass-balance to the ratio of each enzyme species with respect to the initial total enzyme concentration, yields

$$E = 1 - ES - EI - EI^*$$ **Eq. S9**

Given that a fraction of the enzyme will be degraded and re-synthesized every hour (target turnover), **Eq. S9** can be converted to the following equation,

$$1 + \rho * t = E + ES + EI + EI^*$$ **Eq. S10**

where ρ is the fraction of enzyme that is turned over every hour

Under the steady state approximation, $\frac{dES}{dt} = 0$, therefore:

$$[E] = \frac{K_m}{[S]} * [ES]$$ **Eq. S11**

Assuming rapid-equilibrium for initial enzyme-inhibitor complex formation,

$$[EI] = \frac{[I]}{K_i} * [E]$$

so that

$$[EI] = \frac{[I]}{K_i} * \frac{K_m}{[S]} * [ES] \qquad \textbf{Eq. S12}$$

Substitution into **Eq. S10** with the terms containing [ES] in **Eq. S11 and S12**, yields:

$$1 + \rho * t = \frac{K_m}{[S]} * ES + ES + \frac{[I]}{K_i} * \frac{K_m}{[S]} * [ES] + EI^*$$

$$1 + \rho * t = \left(1 + \frac{K_m}{[S]} + \frac{[I]}{K_i} * \frac{K_m}{[S]}\right) * ES + EI^*$$

$$\left(1 + \frac{K_m}{[S]} + \frac{[I]}{K_i} * \frac{K_m}{[S]}\right) = \beta \; and \; \frac{K_m}{[S]} = M$$

$$1 + \rho * t = \beta * ES + EI^* \qquad \textbf{Eq. S13}$$

Derivatization of both sides gives:

$$\rho = \beta * \frac{dES}{dt} + \frac{dEI^*}{dt} \qquad \textbf{Eq. S14}$$

According to **Scheme S2**:

$$\frac{dEI^*}{dt} = k_5 * EI$$

Replacing $\frac{dEI^*}{dt}$ in **Eq. S14** with the above definition, and EI with the definition in **Eq. S12** and EI* with its equality presented in the **Eq. S13**, we have,

$$\rho = \beta * \frac{dES}{dt} + k_5 * \frac{[I]}{K_i} * \frac{K_m}{[S]} * [ES]$$

By rearrangement:

$$\frac{dES}{dt} = \frac{\rho}{\beta} - \left(\frac{k_5}{\beta} * \frac{[I]}{K_i} * \frac{K_m}{[S]}\right) * ES$$

Considering $\left(\frac{k_5}{\beta} * \frac{[I]}{K_i} * \frac{K_m}{[S]}\right) = k$

$$\frac{dES}{dt} = \frac{\rho}{\beta} - k * ES$$

Integration of the above equation gives:

$$ES = \frac{\rho}{\beta * k} + \gamma * e^{-k*t}$$ **Eq. S15**

where $\gamma = ES_0 - \frac{\rho}{\beta * k}$

Assuming that all non-ES forms of the enzyme complexes are representative of the occupied form of the enzyme, we have:

$$TO^t = \frac{1 + \rho * t - ES}{1 + \rho * t} = 1 - \frac{\frac{\rho}{\beta * k} + \gamma * e^{-k*t}}{1 + \rho * t}$$ **Eq. S16**

Note that the inhibitor concentration in the above equations, [I], is either the extracellular concentration in the cell-based experiments or the plasma free fraction of the drug and that K_i is K_i^{app}, which is measured based on drug total concentration in cellular assay or plasma free fraction *in vivo*.

To calculate target occupancy, drug concentration was incorporated into **Eq. S16** by incorporating a multi-dose PK model. Target occupancy was then used in the following equation (**Eq. 17**) to predict drug efficacy (in **Mathematica**) together with a sigmoidal term relates target occupancy and efficacy (target vulnerability):

$$\frac{dAD}{dt} = k_{inf} * \left(1 - \left(\frac{(TO^t)^n}{(TO^t)^n + (TO_{50})^n}\right)\right) * (AD - AD_0)$$ **Eq. S17**

k_{inf} is a rate constant for the change in AD (h^{-1}) while AD is the ankle diameter in mm. AD_0 is the ankle diameter in healthy rats, TO_{50} is the target occupancy that results in 50 percent of the maximum efficacy and n is the Hill coefficient that defines how steeply target occupancy and efficacy are correlated.

Inclusion of BTK inhibitor residence time in the mechanistic PK/PD model
To evaluate the impact of residence-time of reversible BTK inhibitors on the dynamics of target engagement and efficacy we need to include the BTK-inhibitor dissociation rate constant (k_6) in the model (**Scheme S3**).
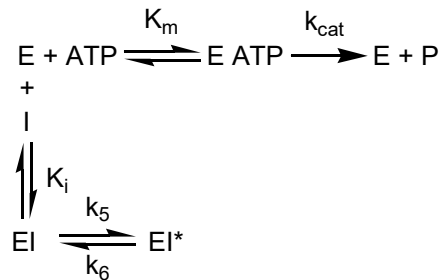
Scheme S3. Kinetic scheme for the reaction of BTK with a reversible competitive inhibitor.

Eq. S7 and **S8** can be modified to include k_6, leading to modified versions of **Eq. S15** and **S16**.

$$\frac{dE.I}{dt} = k_3 * \rho m * [I] * E_t - k_4 * EI - k_5 * EI + k_6 * EI^*$$

Eq. S18 (modified version of **Eq. S7**)

$$\frac{dE.I^*}{dt} = k_5 * EI - k_6 * EI^*$$

Eq. S19 (modified version of **Eq. S8**)

According to **Eq. S14**, we have

$$\rho = \beta * \frac{dES}{dt} + \frac{dEI^*}{dt}$$

Replacing EI* in the above equation with the definition in **Eq. S19**, and EI with the definition in **Eq. S12** and EI* with the definition in **Eq. S13**, we have,

$$\rho = \beta * \frac{dES}{dt} + k_5 * \frac{[I]}{K_i} * \frac{K_m}{[S]} * [ES] - k_6 * (1 + \rho * t - \beta * ES)$$

By rearrangement:

$$\frac{dES}{dt} = \frac{\rho + k_6}{\beta} + k_6 * \rho * t - \left(\frac{k_5}{\beta} * \frac{[I]}{K_i} * \frac{K_m}{[S]} + k_6 \right) * ES$$

Assuming that $\left(\frac{k_5}{\beta} * \frac{[I]}{K_i} * \frac{K_m}{[S]} + k_6 \right) = k$, then

$$\frac{dES}{dt} = \frac{\rho + k_6}{\beta} + \frac{k_6}{\beta} * \rho * t - k * ES$$

Integration of the above equation gives

$$ES = \frac{\rho + k_6}{\beta * k} - \frac{k_6 * \rho}{\beta * k^2} + \frac{k_6}{\beta * k} * \rho * t + \gamma * e^{-k*t}$$

Eq. S20 (modified version of **Eq. S15**)

Where

$$\gamma = ES_0 - \frac{\rho + k_6}{\beta * k} + \frac{k_6 * \rho}{\beta * k^2}$$

Assuming that all non-ES forms of the enzyme represent occupied, inhibited enzyme, we have,

$$TO^t = \frac{1 + \rho * t - ES}{1 + \rho * t} = 1 - \frac{\frac{\rho + k_6}{\beta * k} - \frac{k_6 * \rho}{\beta * k^2} + \frac{k_6}{\beta * k} * \rho * t + \gamma * e^{-k*t}}{1 + \rho * t}$$

Eq. S21 (modified version of **Eq. S16**)

Incorporation of **Eq. S21** together with a multi-dose one-compartment PK model into **Eq. S17** allows the efficacy of a reversible competitive BTK inhibitor to be predicted.

Inclusion of self-limitation term into the kinetics-driven PK/PD model

The rat CIA model shows spontaneous remission after 4 days. Using the same approach as that described by Liu et al.(1) we included a rate constant for self-resolution of the disease (k_{out}) into a modified version of the PK/PD model (**Eq. S23**). The transit model used to derive **Eq. S23** is shown below (**Scheme S4**):
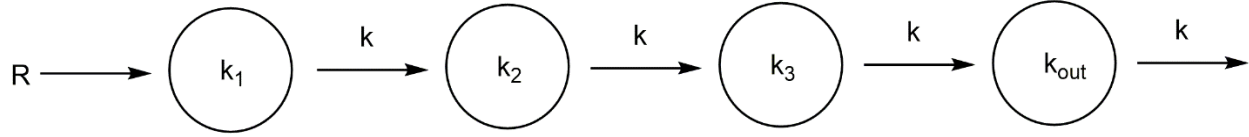
Scheme S4. Transit model used to obtain k_{out}

$$\frac{dAD}{dt} = k_{inf} * \left(1 - \left(\frac{(TO^t)^n}{(TO^t)^n + (TO_{50})^n}\right)\right) * (AD - AD_0) - k_{out} * (AD - AD_0) \qquad \text{Eq. S23}$$

$$\frac{dk_1}{dt} = R - k * k_1 \qquad \text{Eq. S24}$$

$$\frac{dk_2}{dt} = k * k_1 - k * k_2 \qquad \text{Eq. S25}$$

$$\frac{dk_3}{dt} = k * k_2 - k * k_3 \qquad \text{Eq. S26}$$

$$\frac{dk_{out}}{dt} = k * k_3 - k * k_{out} \qquad \text{Eq. S27}$$

AD_0, is a correction factor for the absolute value of AD. The derivatives for k_1 to k_{out} represent the development of the self-resolution process over time. The term R in **Eq. S24** is the initial rate of decrease in ankle swelling before the self-resolution process starts. The transit rate constant, k, governs the transition from k_1 to k_{out}, where k_{out} is the ultimate rate constant that describes the decrease in ankle swelling.

The initial values of k_1, k_2, k_3 and k_{out} at time 0 are 0.

Values of AD_0, k and k_{inf}, were estimated by fitting the untreated (control) experimental data, $TO^t = 0$, to Eq. **S23- S27**, using a value of R = 0.001 h^{-2} taken from Liu et al. (Table 3).(1) This gave AD_0 (mm) 1.78, k (h^{-1}) 0.012 and k_{inf} (h^{-1}) 0.0031.

Eq. S23 was then used to simulate efficacy using the values of AD_0, k and k_{inf}, TO^t from **Eq. S16** and drug concentration from a multi-dose one-compartment PK model.

Supplementary Tables
Table S1. The Fraction of Btk in Total Protein in Ramos Cells

[CC-292] (nM)	Fraction of Btk in total protein (%)	Std. Dev.
0	3.70	1.62
0.4	2.84	1.46
1.5	2.86	1.81
5.9	2.41	1.46
11.7	2.46	1.68
93.8	2.50	1.60
750	3.56	3.01
3000	1.34	0.57

Table S2. The Change in the Fraction of Btk in Total Protein in Ramos Cells as a Function of Time

Time after Drug Washout (h)	Fraction of Btk in total protein (%)	Std. Dev.
0	3.80	2.69
2	3.07	0.49
18	3.23	0.57
24	2.89	0.45

Table S3. Pharmacokinetic parameters for CC-292 in rats[a]

In vivo data							
Dose (mg kg^{-1})	C_{max} (ng mL^{-1})	t_{max} (min)	$t_{1/2}$ (h)	k_a (h^{-1})	k_e (h^{-1})	V_d/F (L kg^{-1})	CL/F (L h^{-1} kg^{-1})
3	235	30	0.7	3.5	1	8	8
30	1003	40.2	1.2	3	0.6	20	12
100	2979	36	9	8.5	0.08	32	2.4

[a]C_{max}, maximum plasma concentration of CC-292; t_{max}, time at which the maximum plasma concentration was observed; $t_{1/2}$, half-life of CC-292; k_a and k_e, rates of absorption and elimination of CC-292, respectively; V_d/F, apparent volume of distribution; Cl/F, apparent clearance.
CC-292 is 92% protein bound.

In vitro **data**: CC-292, free fraction of drug (fu) = 0.08

Supplementary Figures
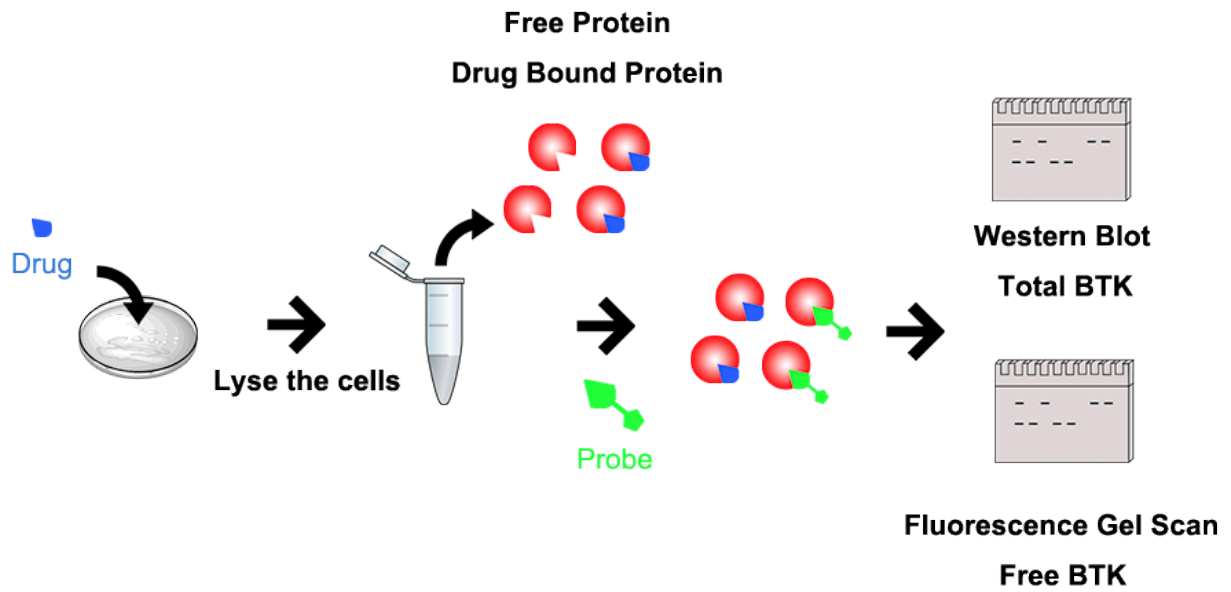
Figure S1. Method for experimentally quantifying target occupancy
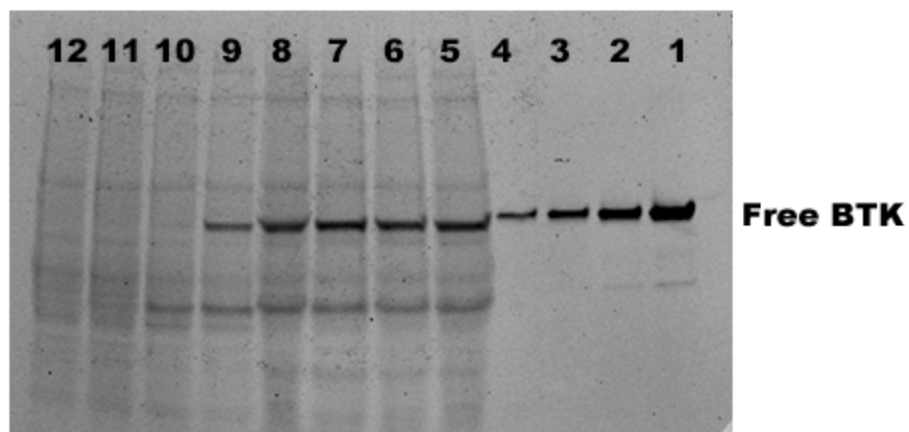
Figure S2. SDS-PAGE analysis of Btk engagement. Treatment of Ramos cells with varying concentrations of CC-292 resulted in alteration in fluorescence intensity of BDP-CC-292 bound to Btk whereas the luminescence from the western blot remained constant.

Fluorescence

13 12 11 10   9   8   7   6   5   4   3   2   1

Free BTK

Western Blot

Total BTK

1. 97.5 ng Pure BTK   5 to 7: 2 hours post drug treatment
2. 48.75 ng Pure BTK   8 to 10: 18 hours post drug treatment
3. 24.38 ng Pure BTK   11 to 13: 24 hours post drug treatment
4. 12.19 ng Pure BTK

Figure S3. *In vitro* Btk Turnover in Ramos Cells. SDS-PAGE showing the increase in fluorescence of the BDP-CC-292 probe as a function of time after CC-292 washout and also showing a western blot of total Btk.

a

Fluorescence

1. 0 h-1;   2. 3 mg/kg 4h-1;   3. 100 mg/kg 4 h-1;
4. 100 mg/kg 4h-2;   5. 100 mg/kg 4h-3;   6. 100 mg/kg 8h-1;
7. 100 mg/kg 8h-2;   8. 100 mg/kg 8h-3

b

Fluorescence

1. 0 h-2;   2. 3 mg/kg 4h-2;   3. 3 mg/kg 4 h-3;
4. 3 mg/kg 8h-1;   5. 3 mg/kg 8h-2;   6. 3 mg/kg 8h-3;

c

Fluorescence

1. 0 h-3;   2. 3 mg/kg 18h-1;   3. 3 mg/kg 24 h-1;
4. 100 mg/kg 18h-1;   5. 100 mg/kg 24h-1;
6. 30 mg/kg 18h-1;

d

Fluorescence

1. 0 h-4;   2. 3 mg/kg 18h-2;   3. 3 mg/kg 24 h-2;
4. 100 mg/kg 18h-2;   5. 100 mg/kg 18h-2;
6. 30 mg/kg 18h-2;

e

Fluorescence

1. 0 h-5;   2. 3 mg/kg 18h-3;   3. 3 mg/kg 24 h-3;
4. 100 mg/kg 18h-3;   5. 100 mg/kg 18h-3;
6. 30 mg/kg 18h-3;

f

Fluorescence

1. 48.75 ng Btk;   2. 0h-6;   3. 0h-7;   4. 30 mg/kg 4h-1;
5. 30 mg/kg 4h-2; 6. 30 mg/kg 4h-3; 7. 30 mg/kg 8h-1; 8. 30 mg/kg 8h-2;
9. 30 mg/kg 8h-3; 10. 30 mg/kg 24h-1; 11. 30 mg/kg 24h-2;

Figure S4. *In vivo* Btk Turnover in B Cells. SDS-PAGE showing the increase in fluorescence of the BDP-CC-292 probe as a function of time after CC-292 washout and also showing a western blot of total Btk.
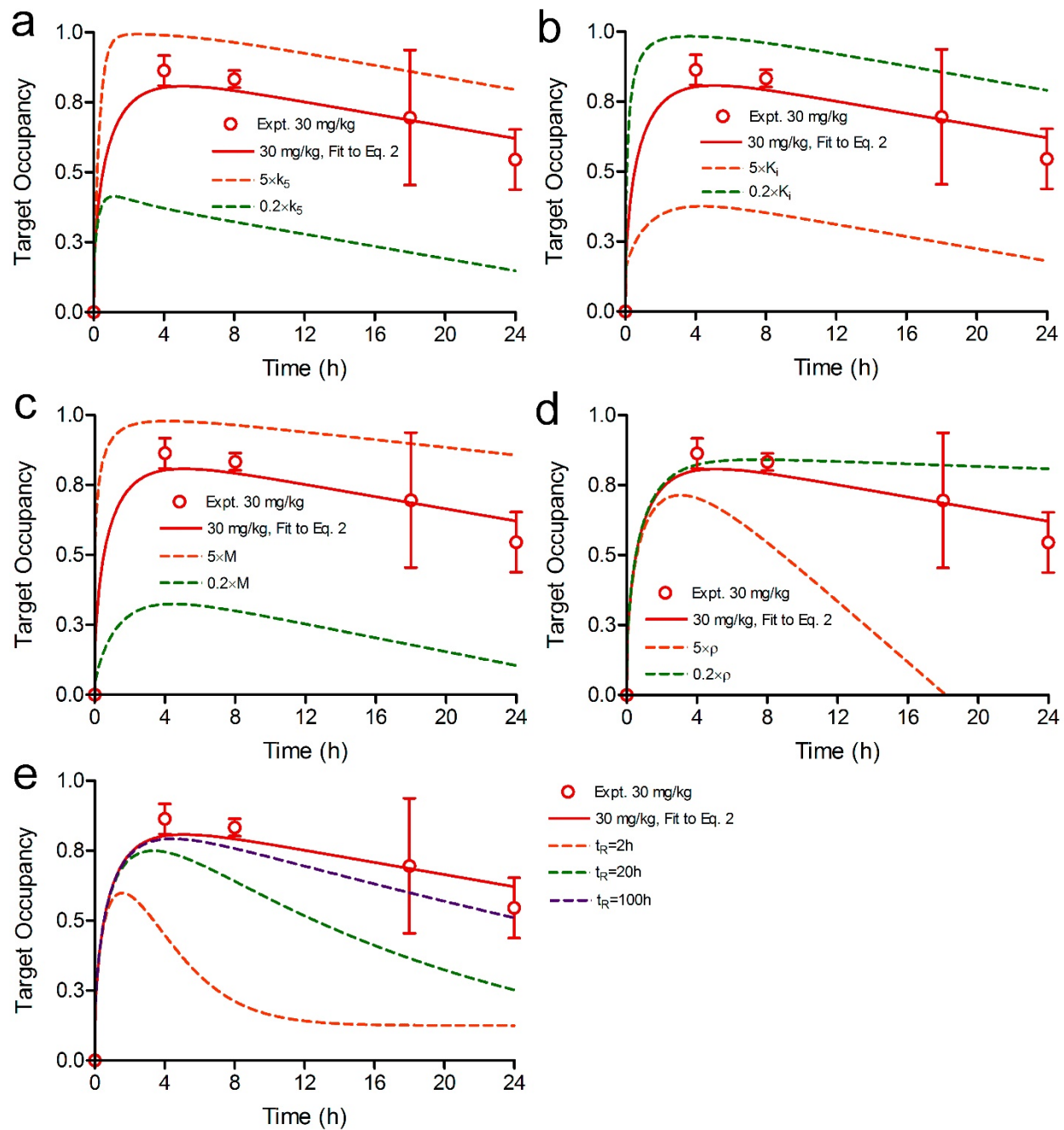
Figure S5. Sensitivity of simulated target occupancy to the values of k_5, K_i, ρ, M and t_R. The experimentally determined *in vivo* target occupancy is shown in red points and the result of fitting to the target occupancy model is shown as a red solid line. In each case the target occupancy has been simulated after increasing or decreasing each parameter by a factor of 5. a) k_5, b) K_i, c) M, d) ρ, e) t_R.

Compound Characterization

Demethylated CC-292 (1) ^1H NMR

^{1}H NMR (400 MHz, METHANOL-d_4) δ ppm 3.85 (t, J=4.80 Hz, 2 H) 4.00 (t, J=4.80 Hz, 2 H) 5.78 (dd, J=9.41, 2.13 Hz, 1 H) 6.33 - 6.40 (m, 1 H) 6.40 - 6.48 (m, 1 H) 6.80 - 6.86 (m, 2 H) 7.25 - 7.30 (m, 1 H) 7.38 - 7.45 (m, 4 H) 7.87 (d, J=4.02 Hz, 1 H) 8.05 (t, J=2.00 Hz, 1 H)
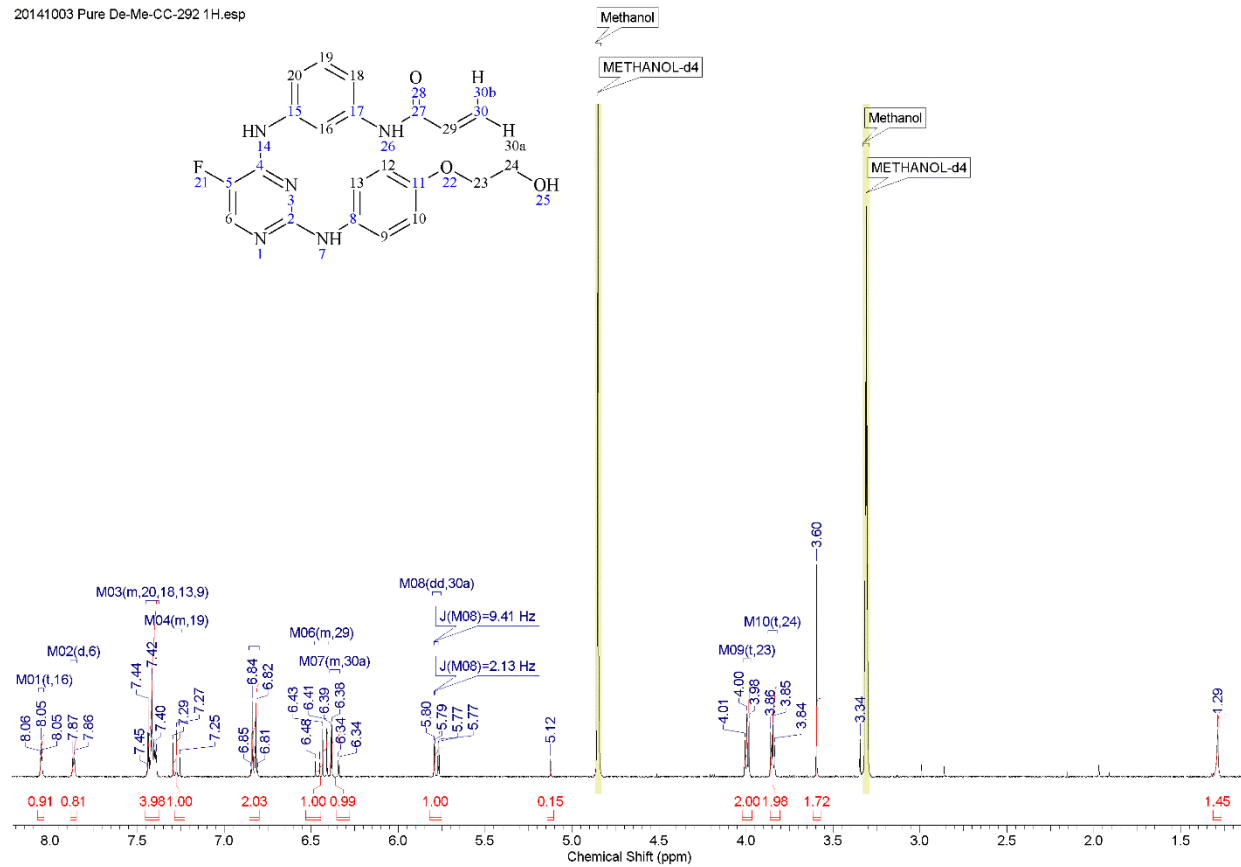
Demethylated CC-292 (1) ^{19}F NMR
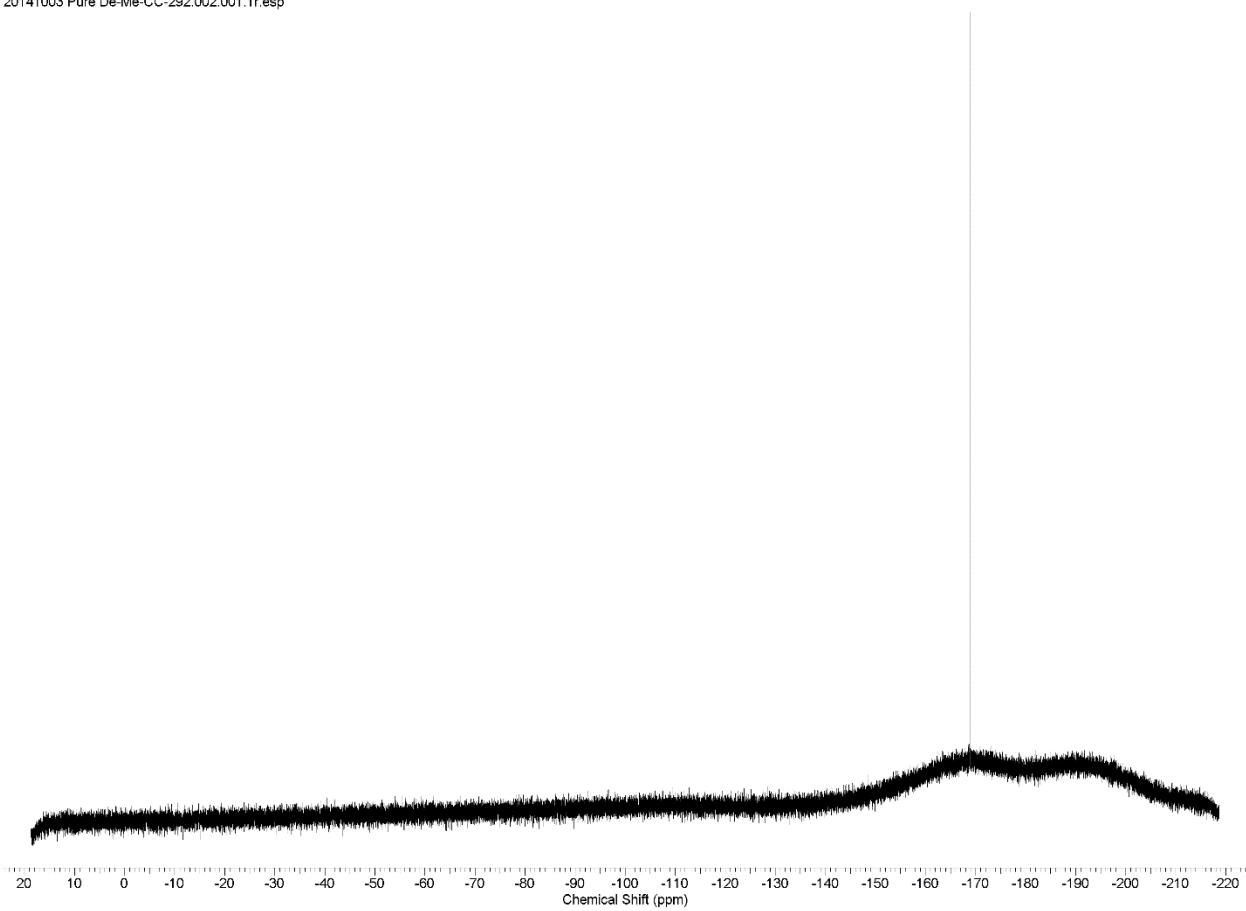
Azido-CC-292 (3) *¹H NMR*

¹H NMR (400 MHz, METHANOL-*d₄*) δ ppm 3.57 (t, *J*=4.90 Hz, 2 H) 4.12 (t, *J*=4.80 Hz, 2 H) 5.80 (dd, *J*=9.54, 2.26 Hz, 1 H) 6.35 - 6.41 (m, 1 H) 6.42 - 6.50 (m, 1 H) 6.82 - 6.86 (m, 2 H) 7.29 (t, *J*=7.90 Hz, 1 H) 7.39 - 7.50 (m, 4 H) 7.89 (d, *J*=3.89 Hz, 1 H) 8.08 (t, *J*=2.01 Hz, 1 H)

20141003 Pure azide-cc-292 probe 1h.esp
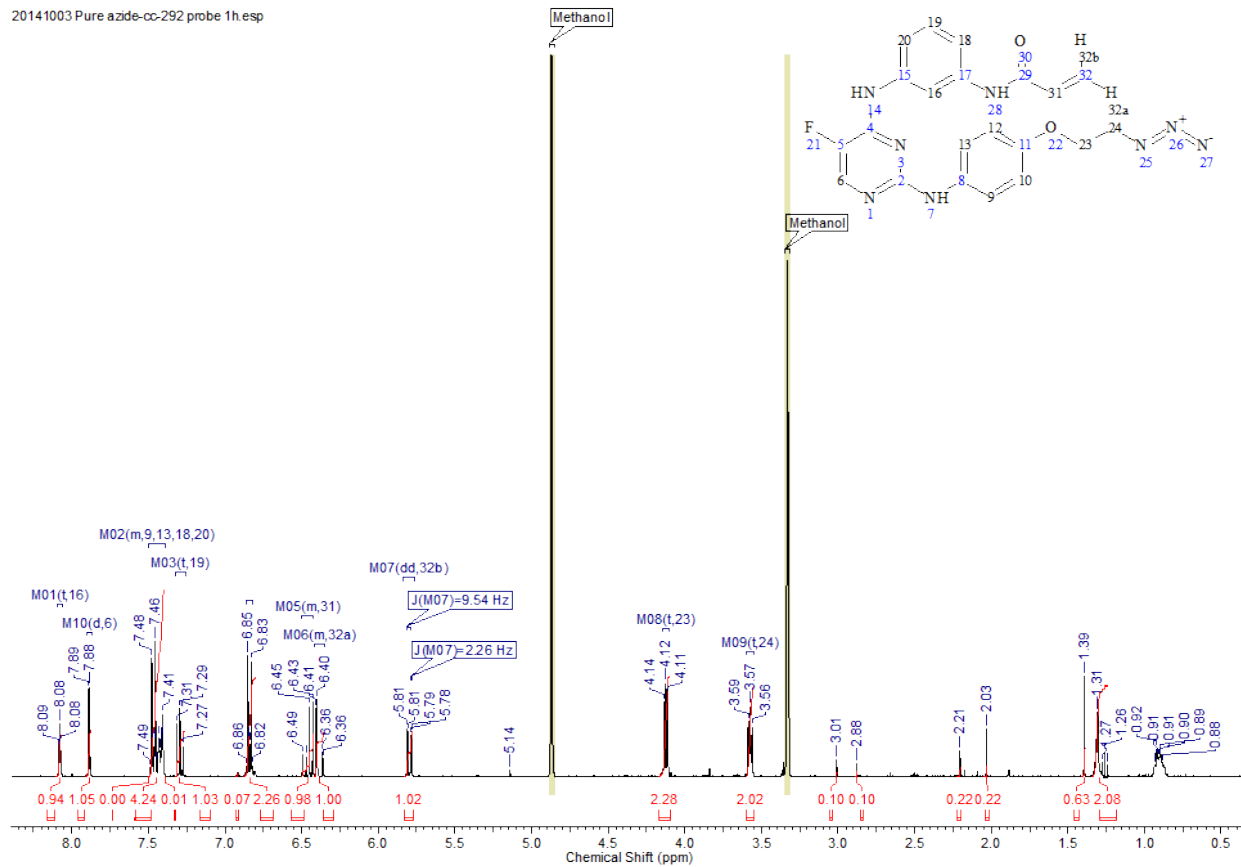
Azido-CC-292 (3) *¹⁹F NMR*

^{19}F NMR (376 MHz, METHANOL-d_4) δ ppm -168.74 (d, J=4.09 Hz, 1 F)

20141003 Pure azide-cc-292 probe 19f.esp
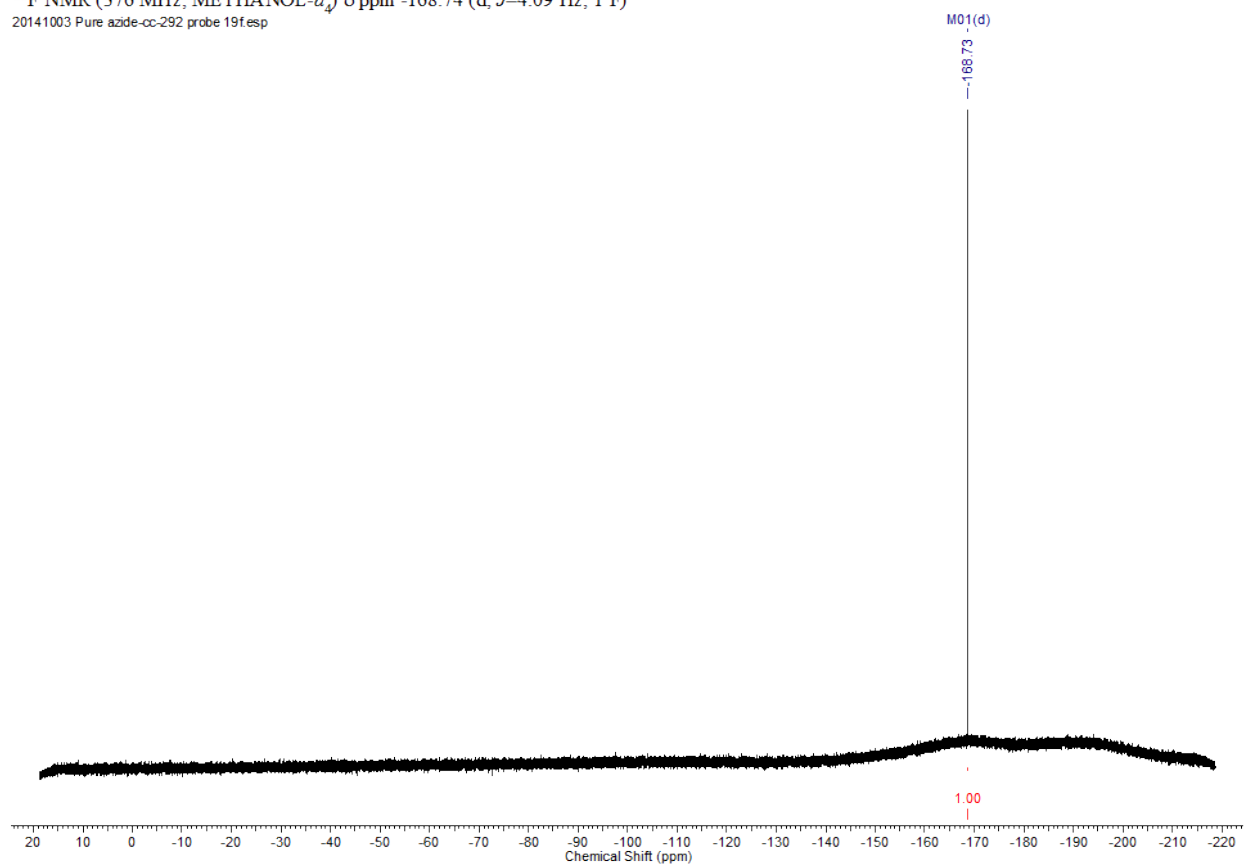
Azido-CC-292 (3) ^{13}C NMR

^{13}C NMR (126 MHz, METHANOL-d_4) δ ppm 50.04 (s, 1 C) 67.27 (s, 1 C) 113.78 (s, 1 C) 114.30 (s, 1 C) 115.41 (s, 1 C) 117.62 (s, 1 C) 121.39 (s, 1 C) 126.58 (s, 1 C) 128.55 (s, 1 C) 131.13 (s, 1 C) 134.07 (s, 1 C) 138.49 (s, 1 C) 139.12 (s, 1 C) 139.47 (d, J=20.89 Hz, 1 C) 140.69 (d, J=246.14 Hz, 1 C) 150.55 (d, J=10.90 Hz, 1 C) 153.86 (s, 1 C) 156.17 (d, J=2.73 Hz, 1 C) 164.72 (s, 1 C)

20141003 Pure CC-292 Azide Probe 13C.esp

S20
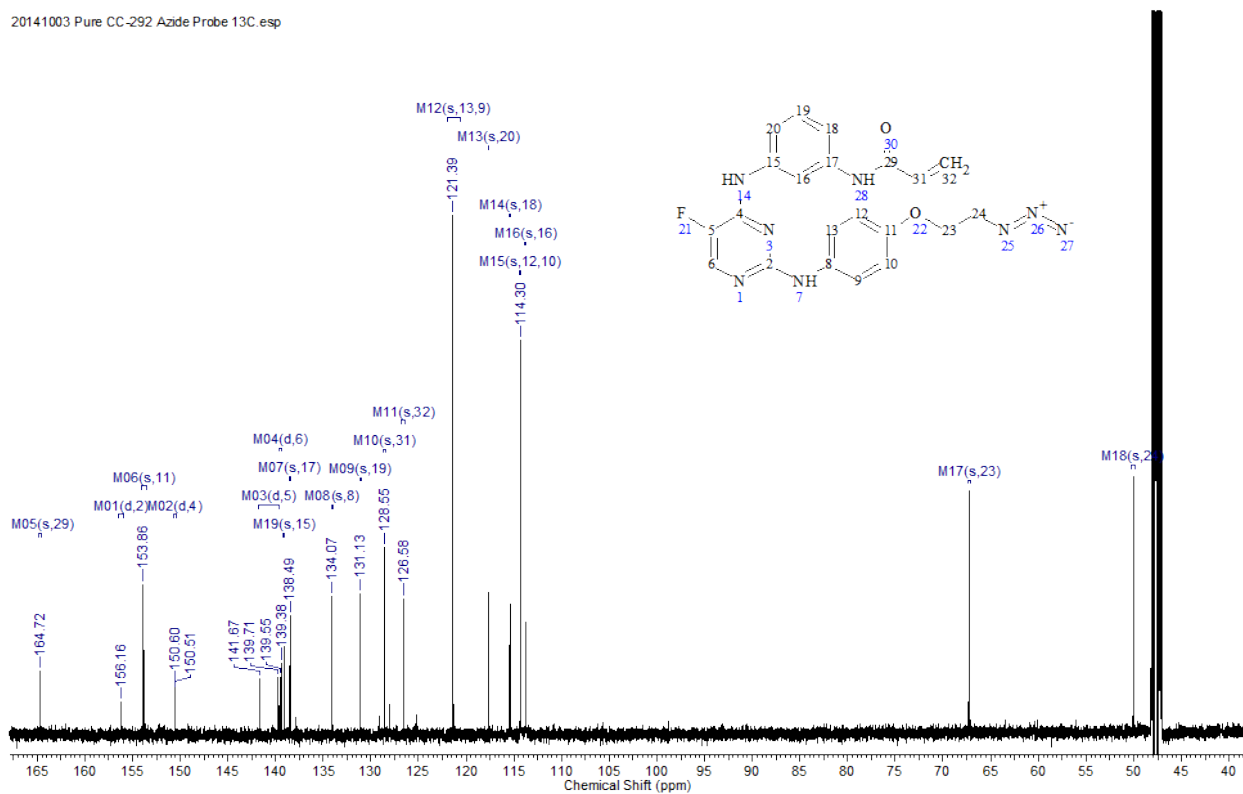
BDP-CC-292 (5) ESI Mass

*MSD1 SPC, time=0.160:0.611 of D:\CHEM32\DATA\TONGE\20150821 BDPP4 POS.D   ES-API, Pos, Scan, Frag: 70

Max: 4033

BDP-CC-292 (5) HRMS

x10 3   Cpd 1: C38 H37 B F3 N11 O3: + FBF Spectrum (0.218-0.234 min) ZDZ-20160428-dirinj-pos-02.d Subtract

764.3193([C38H37BF3N11O3]+H)+
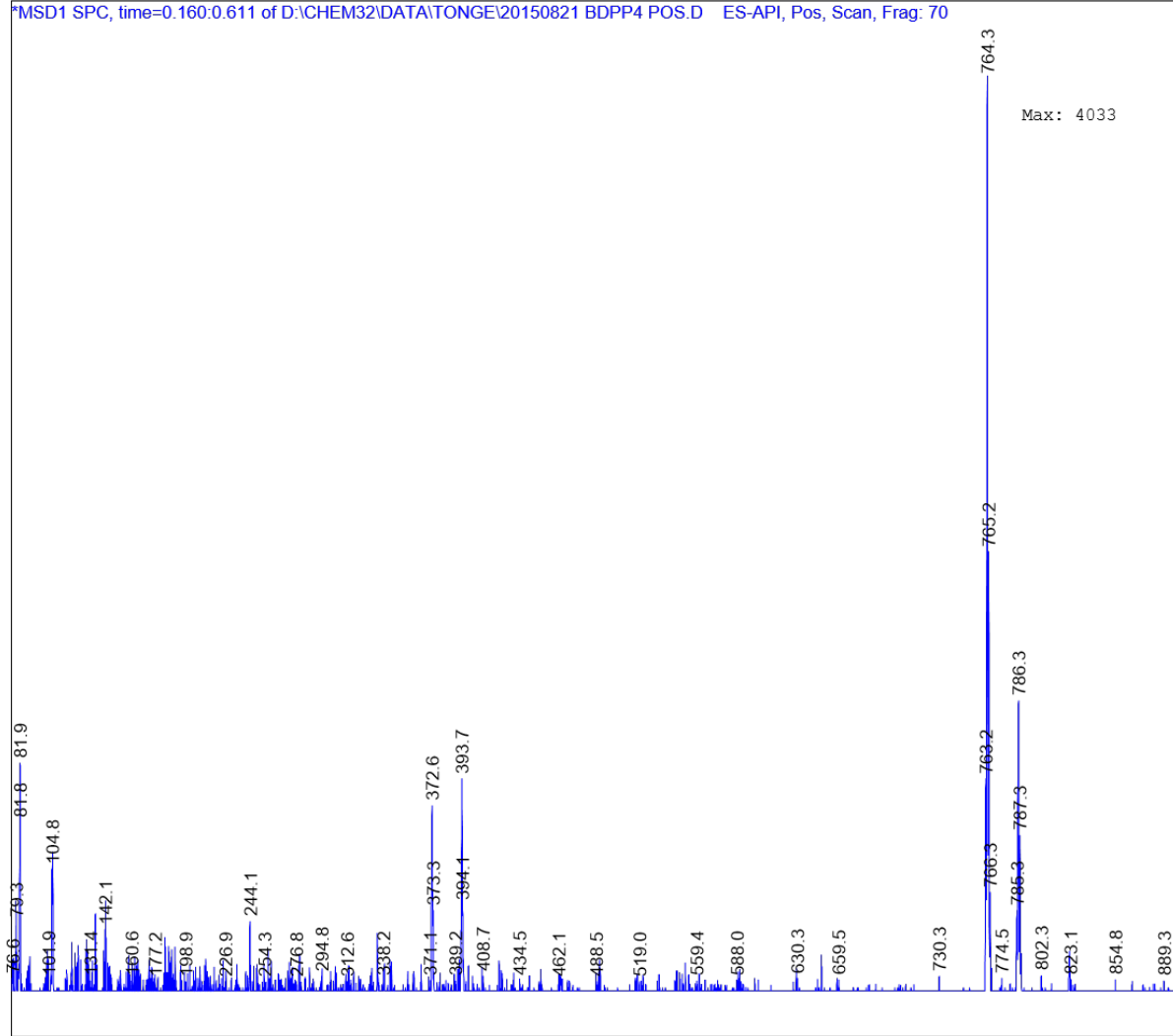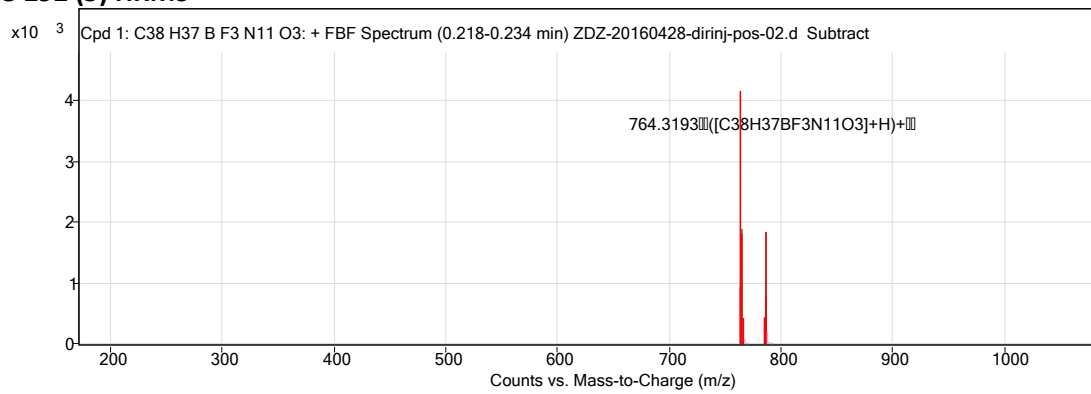
BDP-CC-292 (5) HPLC chromatography

Solvent A: 20 mM Ammonium Acetate

Solvent B: Acetonitrile

—— UV spectra

—— Solvent B Percentage

Product Peak,
Rention Time: 35. 5 to 37.5 min
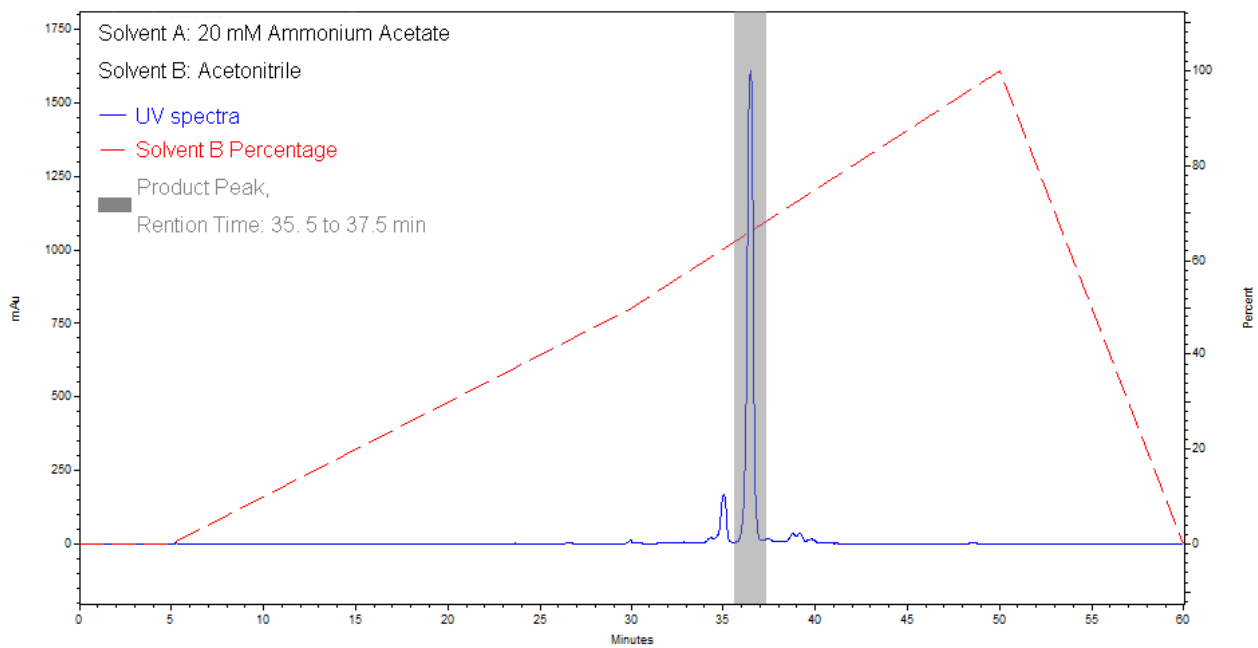
References

1. Liu L*, et al.* (2011) Antiarthritis effect of a novel Bruton's tyrosine kinase (BTK) inhibitor in rat collagen-induced arthritis and mechanism-based pharmacokinetic/pharmacodynamic modeling: relationships between inhibition of BTK phosphorylation and efficacy. *J Pharmacol Exp Ther* 338(1):154-163.